BULLETIN OF THE EARTHQUAKE
RESEARCH INSTITUTE
Vol. 38 (1960), pp. 13-27

2. On the Spectral Structure of Earthquake Waves.

—The Relation between Magnitude and Predominant Period—

By Tosimatu MATUMOTO,

Earthquake Research Institute.

(Read, Dec. 22, 1959.—Received, Dec. 28, 1959.)

Summary

Using the digitalized data processing apparatus, the velocity spectra of *P*-wave part and *S*-wave part were studied for the shocks occurred in the narrow region off shore of north east Honshû, Japan.

As the results, several groups of the predominant period were found corresponding to the maxima appeared in each velocity spectrum, and these periods were related to the magnitude of the shocks as

$$M=\alpha_i+\beta_i \log T_i \ .$$

Comparing the period of the vibration of a spherical shell, the possibility of which the groups of the predominant period were explained as the oscillations of the fundamental and the higher mode of the origin were discussed.

§ 1. Introduction

To attack the nature of earthquake waves, it is very important to know their spectral structure. However, an essential difficulty for this problem is that the seismic wave is not stationary. In such analysis, the time function must be stationary during the time interval of analysis, while the seismic wave is considered not to have such character.

In spite of this restriction, it is found that there are little differences between the spectrum calculated at the finite interval and that of slightly shifted interval if these intervals contain a single wave group or its metamorphosed waves only as described in a later section. In such well selected interval, the change of spectrum is small even if the range of interval is altered to some extent. Therefore Fourier analysis is valid for scuh restricted interval to investigate the spectral structures of earthquake disturbances.

In this paper, Fourier analysis is applied for *P*-wave part and *S*-wave part of shocks which occured in the narrow region off the *E* coast Kinkazan, of off shore of north east Honshû Japan.

§ 2. Tracer and Relay Computer used in this analysis

A few years ago, we made a relay computer designed for correlogram analysis as reported in our previous paper.[1]

When we use this computer the data must be digitalized and punched on the tape in advance. However, it is a troublesome work to measure the disturbance in the seismogram, to obtain the numerical values and then to punch them on the paper tape. To get rid of this work we made a tracer which directly converts the optically recorded seismic disturbance into a digital one.

Since it was not reported in our previous paper we will give a brief description of this instrument.

In this instrument, at first we choose the converting rate of the amplitude between the digital tape and the optical recorded seismogram by the amplitude adjuster according to the amplitude of the original seismic disturbance.

The next step is to put the cross wire of the microscope upon the trace of the record shifting the cross wire by rotating the handle attached at the right side of the instrument. By this operation the amplitude of the record is converted into the angle of rotation of the commutator, and the amplitude is read off in the cyclic-code. Through the cyclic-binary converter, the signal which is propotional to the amplitude of the original disturbance is ready to be sent to the perforator. When the switch is closed, the perforator is operated, and at the same time, the drum on which the seismogram is mounted is driven stepwise by the stepping ratchet.

The time interval of readings on the original seismogram is 0.2 or 1.0 sec, one of which being choosen according to the period involved in the disturbance.

The whole process of the conversion and the calculation is schematically shown in Fig. 2. For the purpuse of Fourier analysis, digitalized Fourier tapes, namely the tapes of sine and cosine functions, are provided. Both the Fourier tape and the digitalized tape are applied to the inputs of the relay computer, and their correlation is calculated.

To get the velocity spectrum of the seismic disturbance, the inverse of the velocity sensitivity of the seismograph are multiplied, and we can get the velocity spectrum of the seismic disturbance.

---

1) Y. SATÔ and T. MATUMOTO, *Bull. Earthq. Res. Inst.*, **34**(1956), 279–281

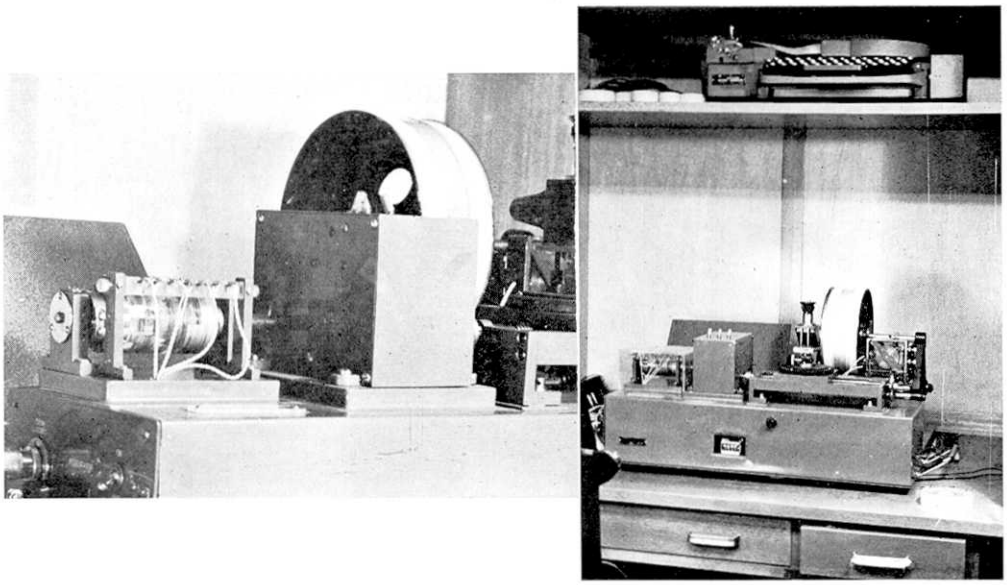

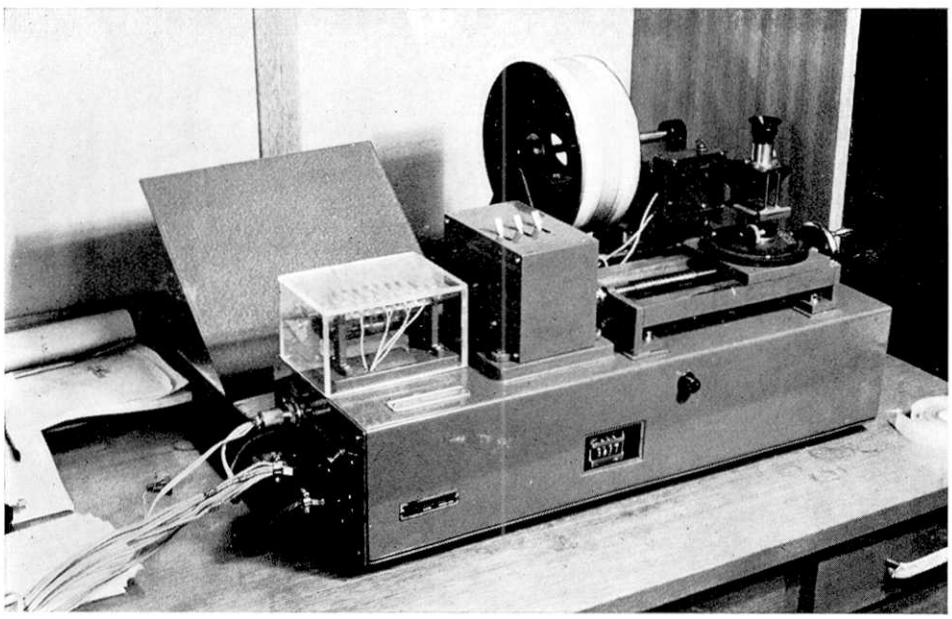

Fig. 1. The tracer by which an analogue seismogram is converted into the digital one.

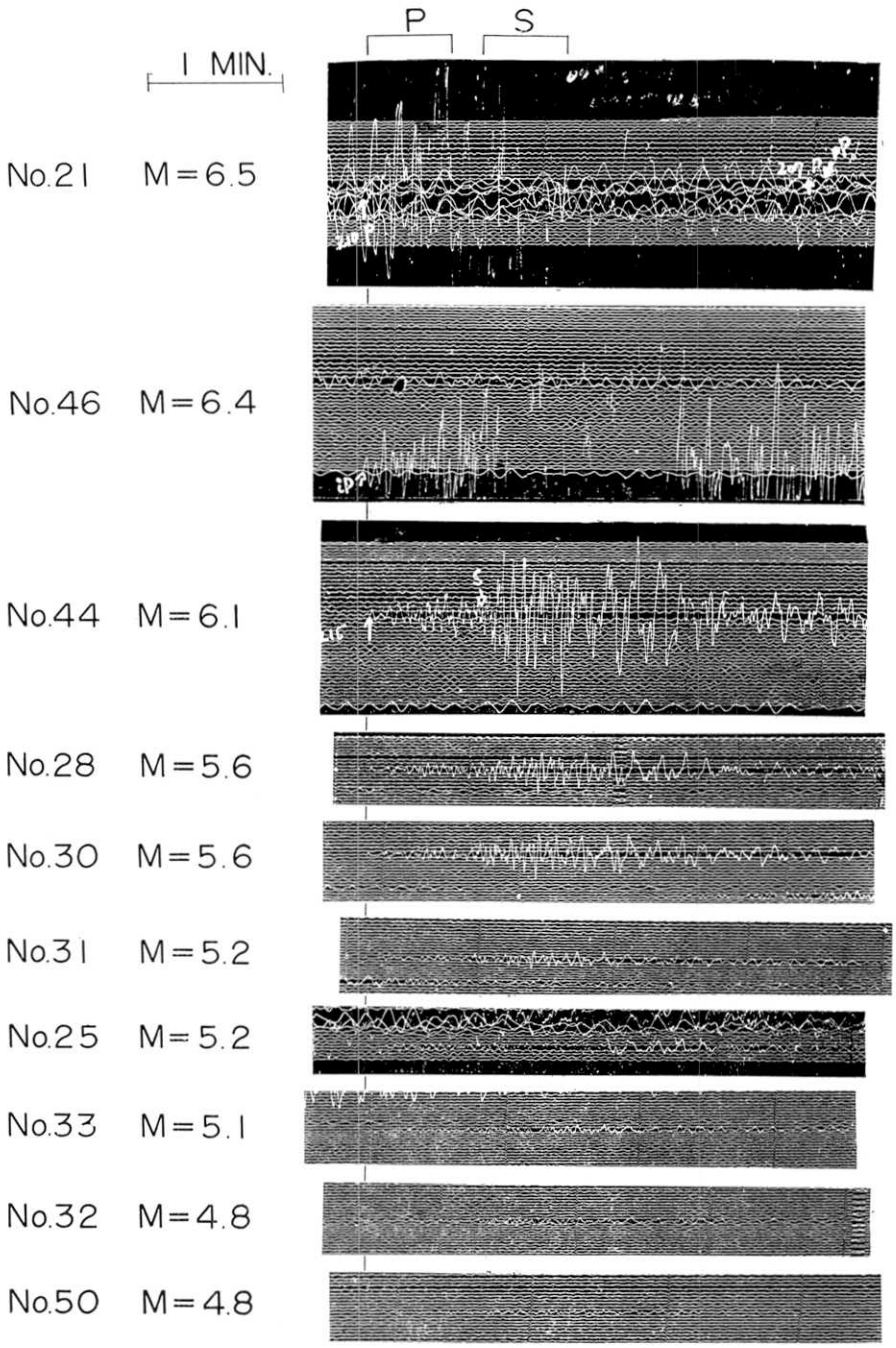

Fig. 3. Seismic Disturbances recorded by vertical HES 1–20 Instrument.

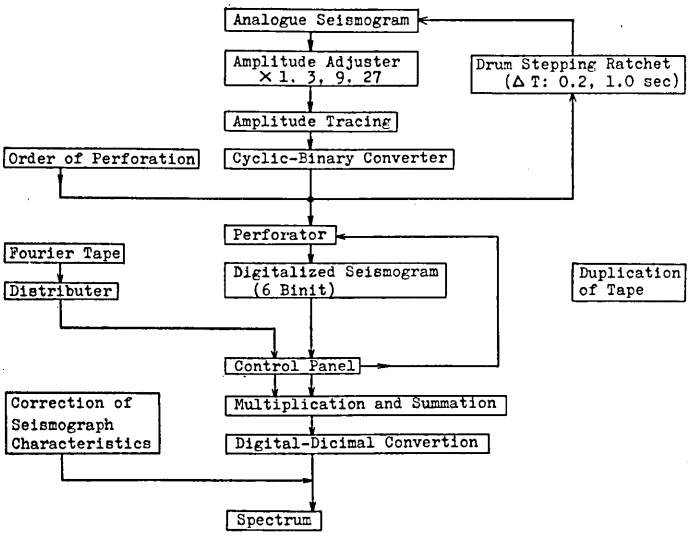

Fig 2. Schematic Illustration of Calculating Process of Spectra.

§ 3. Seismogram used in this Study

The seismograms used in this analysis were obtained at our seismological station located at Mt. Tsukuba.[2]

The serial number, date, location and magnitude of earthquakes are shown in Table 1. Some of these epicenters were determined by J.M.A.

Table 1. The List of Earthquakes Off *E* Coast of Kinkazan

No.	Date			Location	Depth	Magnitude
	April, 1958				km.	
21	07 d	18 h	05 m	38 1/4 *E*, 143 3/4 *N*	20 ca.	6.5
25	07	23	18			5.2
28	08	07	11	38 1/4, 143 3/4	Shallow	5.6
30	08	10	01	38 1/4, 143 3/4	20 ca.	5.6
31	08	15	27			5.2
32	08	16	39			4.8
33	08	17	03			5.1
44	10	11	50	38 1/4, 143 3/4	20 ca.	6.1
46	11	00	58	38 1/2, 1444	20 ca.	6.4
50	11	12	50			4.8

(Japan Meteorological Agency). For smaller earthquakes, however, the epicenters were not given by J.M.A., but it may be reasonable to assume

2) 140° 06′ 36″ E, 36° 12′ 39″ N.

that the epicentral distances are almost the same within the error of a few percent because they have nearly equal P–S duration time. The mean epicentral distance is about 400 km.

The constants and the characteristic curves of the seismographs at Mt. Tsukuba[3] are shown in Table 2 and Fig. 4 respectively.

Table 2. Constants of the Instruments

Mt. Tsukuba

No.		V_{max}	T_1	T_2	h_1	h_2	ρ	σ
			sec	sec.				
1. Hagiwara Inverted Pendulum Seismogrph	(EW)	34	5.0		0.60		0.45	
2. Ditto.	(NS)	34	5.0		0.64		0.47	
3. Ishimoto Acceleration Seismograph	(EW)	200	0.12		0.70		0.05	
4. Ditto.	(NS)	220	0.11		0.58		0.04	
5. Ditto.	(UD)	190	0.10		0.57		0.05	
6.* HES 1-1**	(EW)	29000	1.00	1.16	1.0	1.0	0.1	
7.* Ditto.	(NS)	29000	0.98	1.10	1.0	1.0		0.1
8.* Ditto.	(UD)	37000	0.97	1.26	0.8	1.0		0.1
9.* Anderson-Wood Type Torsion Seismograph	(EW)	2000	0.80		0.8		0.00	
10.* Ditto.	(NS)	2400	0.80		0.8		0.00	
11.* HES 1-20**	(EW)	1740	1.0	22.4	3.1	1.0		0.74
12.* Ditto.	(NS)	1880	1.0	20.7	3.0	1.0		0.73
13.* Ditto.	(UD)	2330	1.0	21.6	2.3	1.0		0.66
14. Columbia Long-Period Seismograph	(EW)	697	15.1	77.	3.1	1.2		0.25
15. Ditto.	(NS)	432	15.1	91.	3.1	1.0		0.26
16. Ditto.	(UD)	627	15.1	104.	1.5	1.1		0.12
17.* HES 1-0.2**	(EW)	144000	1.0	0.24	1.0	0.5		1.0
18.* Ditto.	(NS)	144000	1.0	0.24	1.0	0.5		1.0
19.* Ditto.	(UD)	150000	1.0	0.24	1.0	1.0		0.5

T_1: Period of pendulum.
T_2: Period of galvanometer.
h_1: Damping constant of pendulum when the galvanometer is clamped.
h_2: Damping constant of galvanometer when the pendulum is clamped.
ρ: Solid friction.
σ: Coupling factor.
*: Precise film recording system is adopted.
**: Hagiwara Electromagnetic Seismograph.
Annexed numbers indicate the approximate period in second of pendulum and galvanometer.

3) T. HAGIWARA and T. MATUMOTO, *Monthly Meeting of the Earth Research Institute*, (July, 1959).

The seismograms recorded by the vertical HES 1–20 instrument are shown in Fig. 3, the serial number of earthquakes corresponded to that of Table 1.

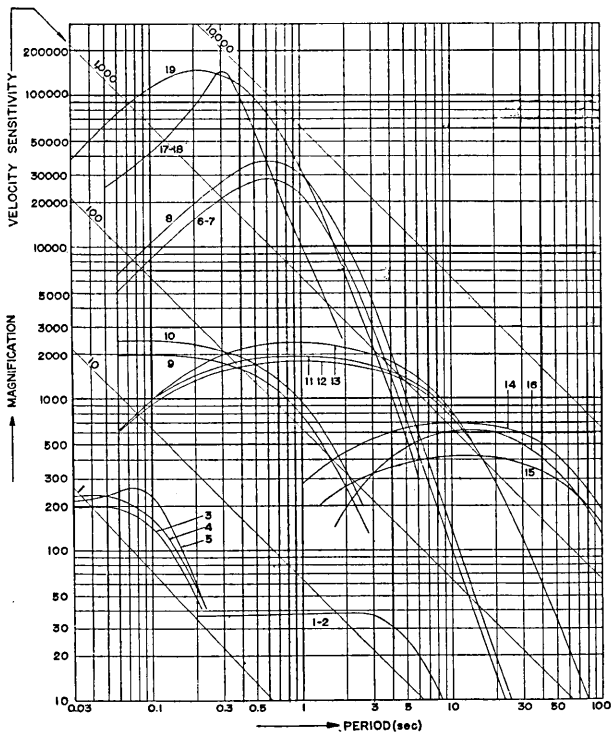

Fig. 4. Characteristic Curves of Seismographs observed at Mt. Tsukuba.

The analysis is performed both for *P*-wave part and *S*-wave part. Starting from the arrival of *P* and *S* phase, 180 sample points are selected on the original seismogram, in which the time interval of succeeding sample points is 0.2 sec each. Thus the range of the analysis in which Fourier coefficients are determined is $0.2\,\text{sec} \times 180 = 36\,\text{sec}$. In these ranges, only *P* (or *S*) wave and its metamorphosed waves are involved. Therefore we call them *P*-wave part and *S*-wave part.

§ 4. The Spectra or *P*-Wave and *S*-Wave Parts

Preceding our study, the analyses were performed for some different intervals which were shifted by several seconds to check the change of Fourier coefficients according to these intervals. The *S*-wave part of No. 44 earthquake, for instance, is analysed for the range of 36 sec from

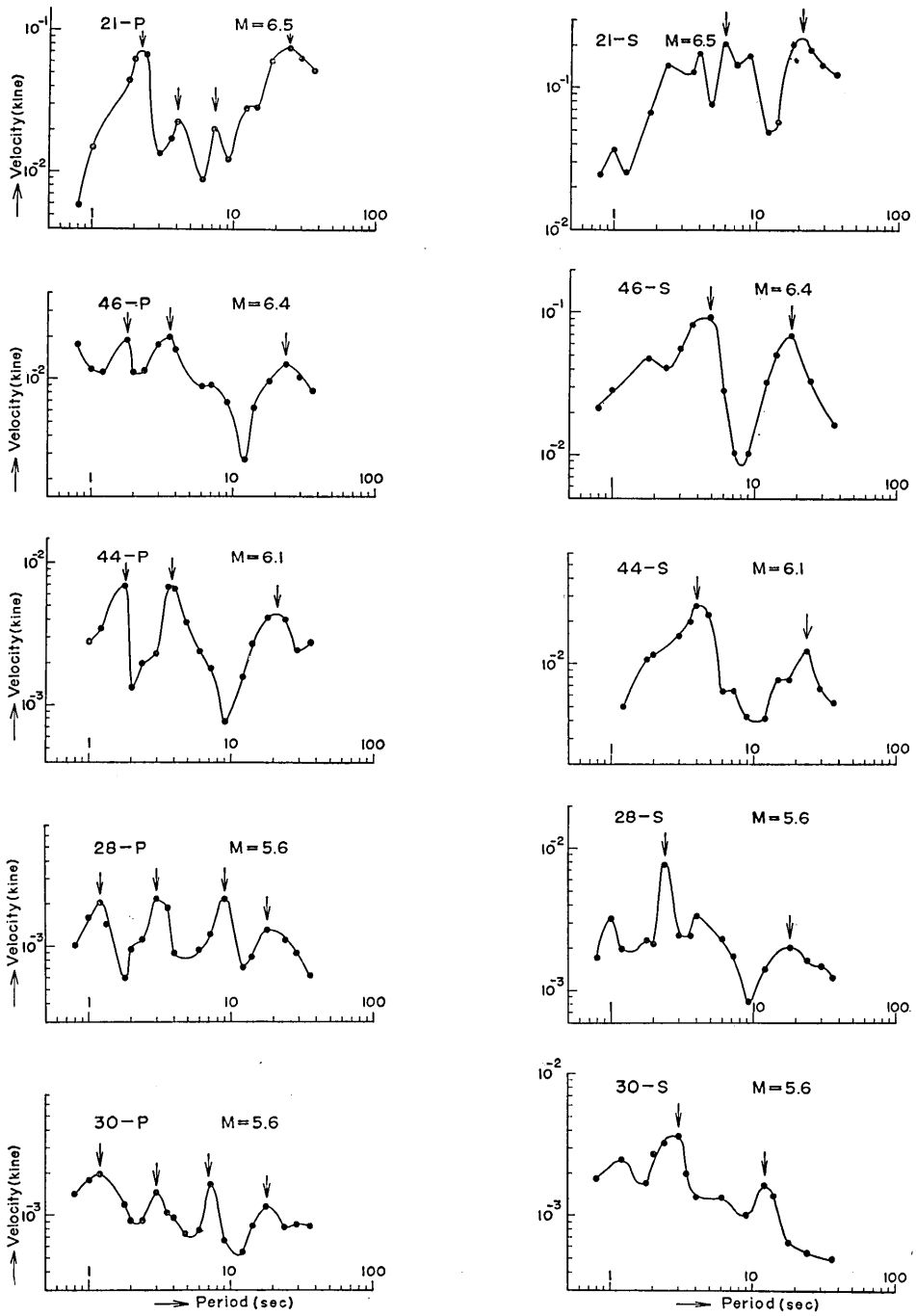

Fig. 7a. Spectra of *P*- and *S*-Wave Parts.

The number of each spectrum is corresponding to the serial number of Earthquakes shown in Table 1.

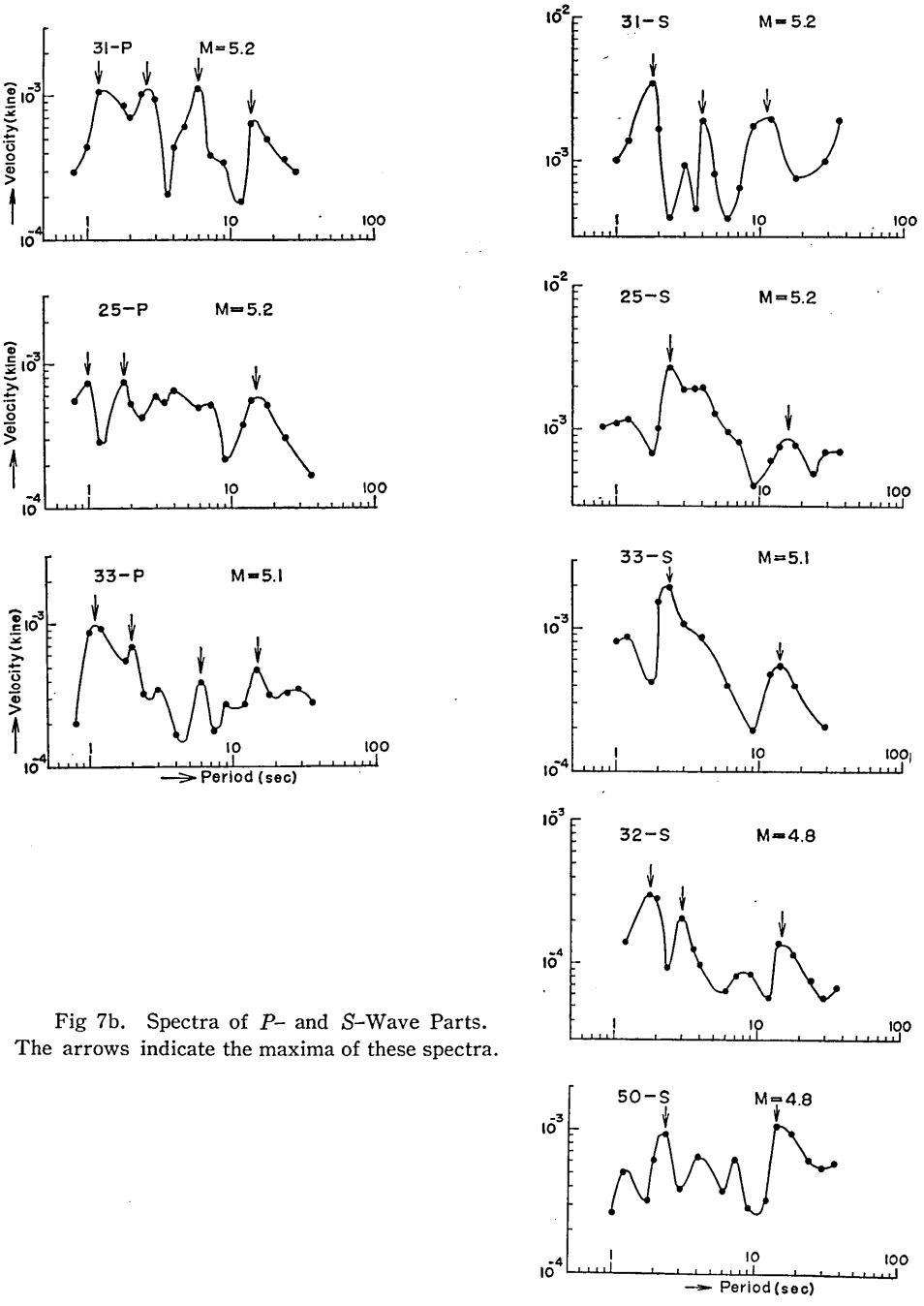

Fig 7b. Spectra of *P*- and *S*-Wave Parts. The arrows indicate the maxima of these spectra.

the commencement of S phase (44-S), from 5 to 41 sec (44-$S1$), and from 10 to 46 sec (44-$S2$). The volocity spectra corresponding to respective interval are shown by black dots, white dots and triangles in Fig. 5.

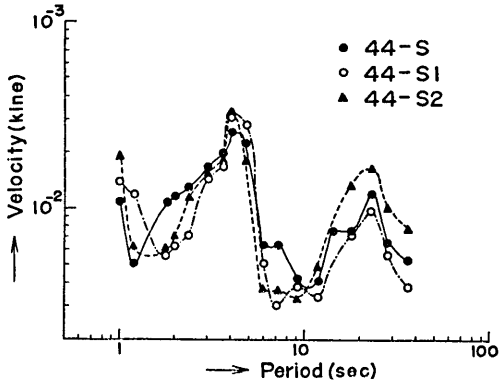

Fig. 5. Similarity of Spectra corresponding to the different Intervals.

These spectra show considerably good coincidence with each other, and the change of spectral feature is small even for the slightly different range of analysis.

In Fig. 6, we can find the similarity of spectra reduced from the records taken by different types of seismographs. This result also proves that the correction of the seismograph is valid within the range used in this analysis.

The velocity spectra of the shocks which are listed in Table 1 are shown in Figs. 7a and 7b.

The main features of these spectra are as follows:

(1) As a whole, the spectra are fairly flat throughout the range of period used in this analysis (1.0-36 sec). In other words, the energy is widely distributed throughout the range of analysis.

(2) To speak precisely, however, there are some maxima in each spectrum. Some of them are remarkable and some of them are not. They are illustrated by the arrows in Fig. 7a and 7b.

(3) It seems there is some relation between the periods corresponding to these maxima and magnitude of the shock, which will be described in the next paragraph.

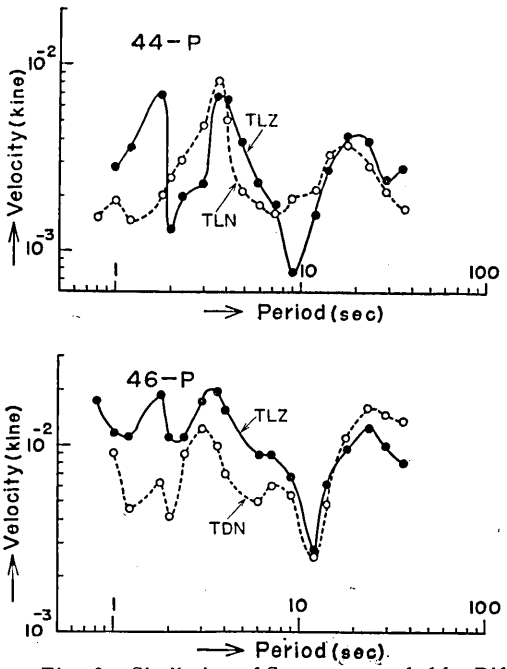

Fig. 6. Similatity of Spectra recorded by Different Type of Seismograph.

§ 5. The Relation between Magnitude and the Predominant Period

The magnitude of the shocks versus logarithm of the predominant periods shows a close relation as illustrated in Figs. 8a and 8b. In

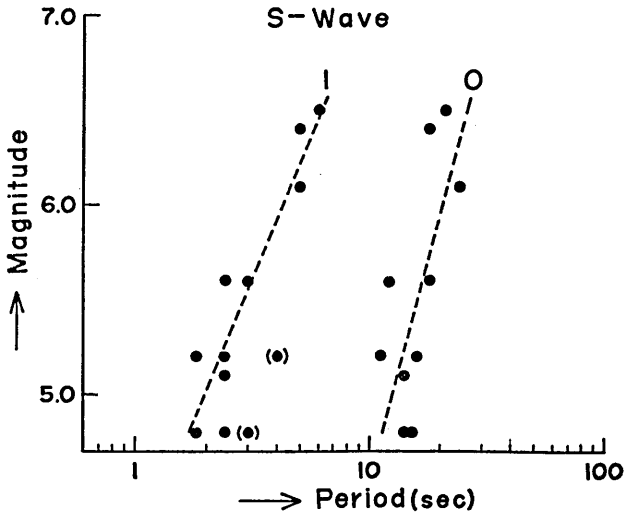

Fig. 8a. Predominant Periods of *S*-Wave Part.

these figures, the predominant periods are clearey separated into several groups. As for *P*-wave part they are separated to three groups and

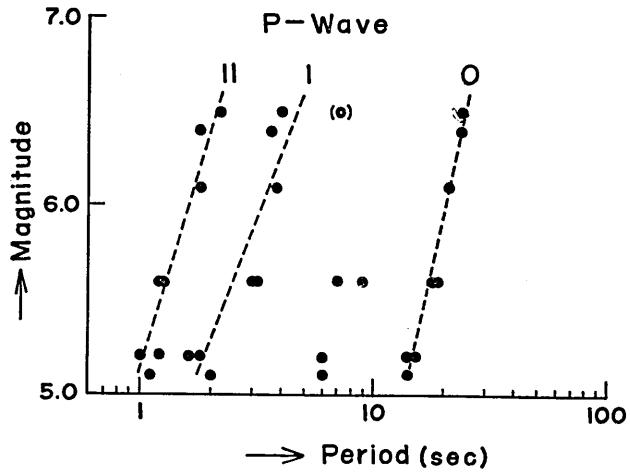

Fig. 8b. Predominant Periods of *P*-Wave Part.

an additional one. These branches are symbolized by the notation 0, I and II as shown in Table 3.

Table 3. Predominant Periods of Spectra

No.	M	P-Wave 0		I.	II.	S-Wave 0.		II
		sec	sec	sec	sec	sec	sec	sec
21	6.5	24.	(7.2)	4.0	2.2	21.		6.0
46	6.4	24.		3.6	1.8	18.		5.0
44	6.1	21.		3.8	1.8	24.		5.0
28	5.6	18.	9.0	3.0	1.2	18.		2.5
30	5.6	18.	7.0	3.0	1.2	12.		3.0
31	5.2	14.	6.0	1.6	1.2	11.	(4.0)	1.8
25	5.2	15.		1.8	1.0	16.		2.4
33	5.1	14.	6.0	2.0	1.1	14.		2.4
32	4.8					15.	(3.0)	1.8
50	4.8					14.		2.4

Also for S-wave part two branches are evident, which are noted by 0 and I.

Assuming the relation

$$M=\alpha_i+\beta_i \log T_i \ , \qquad (1)$$

the values of α_i and β_i are determined by the method of least squares.

The values of the respective branch are shown in Table 4.

Table 4. Relation between Predominant Period T and Magnitude M.
$M=\alpha_i+\beta_i \log T_i$.

Branch		α_i	β_i
P-Wave Part	0	−1.45	5.70
	I	4.31	3.25
	II	5.11	4.27
S-Wave Part	0	0.76	3.97
	I	4.11	3.03

Although there are some deviations among the values of β_i, all branches may be regarded as parallel with each other. This fact suggests that all predominant periods are related to the magnitude of the respective shock, and that the ratio of the predominont periods belonging to the branch 0 and others are constant regardless of the magnitude. It is natural to think that these characteristics of the predominant period are due to the nature of the origin, or in other words, to the mechanism of the occurrence of the earthquake, rather than to the nature of the ray path.

§ 6. Discussion

In the previous section, the nature of the velocity spectra is described. In this section, we want to make some discussion of them.

As the origin model, we take a volume of an arbitrary shape, in which the strain energy is stored, and this energy is transformed to the kinetic energy of seismic wave when the earthquake occurs. The volume of the origin is, therefore, related to the energy of the earthquake, and the period of the seismic wave is determined by the radius (or some related quantity) of the origin.

For instance, we take a spherical shell as the origin model. The period of the vibration of this model was occasionally calculated by us to attack the vibration of the earth.[3]

The calculation was made for the vibration of the first class of this model, which was composed of two parts, namely the core and the mantle. We put the ratio of radii of core and earth's surface as 0.5469. The calculation was performed both for a rigid core and a liquid core, but only the roots of a characteristic equation corresponding to the model of the liquid core is shown in Table 5.

Table 5. The Periods of Vibration of Spherical Shell.
($b/a=0.5469$, Liquid Core, $1/\xi_{n,N}=T_{n,N}V_s/2\pi a$)

	$1/\xi_{n,N}$		
n \ N	0	I	II
0	—	0.1358	0.0709
1	—	0.131	0.0704
2	0.414	0.122	0.0690

In this Table, n denotes the degree of spherical harmonics, and N indicates the number of nodal planes in r-direction. The number $T_{n,N}V_s/a$ is the ratio of the period of oscillation to the time taken by a distortional wave to travel over a distance equal to the diameter of the sphere.

It is important to note that when the value of n is given there are many modes of vibration corresponding to $N=0, 1, 2$ and so on.

The period of each mode is decided by

$$T_{n.N}=\frac{2\pi a}{V_s\xi_{n,N}} \qquad (6)$$

3) T. MATUMOTO and Y. SATÔ, *Bull. Earthq. Res. Inst.*, **32**(1954), 247-258.

In case of $n=2$, for instance, the periods are calculated against the various value of the radius as a shown in Table 6.

Table 6. Radius of Origin and Calculated Periods of Distortional Vibration

Radius a	Period of Distortional Vibration $N=0$	$N=1$	$N=2$
km.	sec.	sec.	sec.
1	0.650	0.192	0.108
2	1.30	0.383	0.217
4	2.60	0.766	0.433
6	3.90	1.15	0.650
10	6.50	1.92	1.08
20	13.0	3.83	2.17
40	26.0	7.66	4.33
60	39.0	11.5	6.50
100	65.0	19.2	10.8

The velocity of the distortional wave is assumed to be 4 km/sec in this calculation. Comparing the observed periods of Table 2 and the values of Table 6, it may be suggested that the periods which belong to the branch I are explained by the vibration of the higher mode ($N=1$). As these periods are deeply affected by the nature of origin, there is a possibility to attack the nature of origin by means of the investigation of the higher mode vibration as well as the fundamental one. In case of P-wave, the branch 0, I and II will be explained by the dilatational vibration of fundamental mode and of higher mode respectively.

Inserting the relation (2) into (1), we get

$$M=\alpha_{n,N}-\beta_{n,N}\log\left(\frac{2\pi}{V_s\xi_{n,N}}\right) \qquad (3)$$

When the values $\alpha_{n,N}\beta_{n,N}$ and $\xi_{n,N}$ corresponding to the fundamental mode are given, the relation between magnitude and the radius of origin is estimated.

In case of $n=2$ and $N=0$, the values are as follows as shown in Table 4 and Table 5:

$$\alpha_{2,0}=0.76\ ,\quad \beta_{2,0}=3.97\ ,\quad \xi_{2,0}=0.414\ .$$

Assuming $V_s=4$ km/sec, we get the following results:

$$M=0.02+3.97\log a\ (\mathrm{km}) \qquad (4)$$

Based on this equation, the relation between M and a is estimated as shown in Table 7.

Table 7. Relation between Magnitude and Radius of Origin.

M	4.0	4.5	5.0	5.5	6.0
$\log a$	1.003	1.129	1.255	1.381	1.507
a (km)	10.1	13.5	18.0	24.1	32.2
M	6.5	7.0	7.5	8.0	8.5
$\log a$	1.633	1.759	1.885	2.011	2.137
a (km)	43.0	57.4	76.8	103.	137.

In conclusion, author expresses his hearty thanks to Prof. T. Hagiwara and Asist. Prof. Y. Satô who gave him useful advices and revised this paper with goodwill.

---

2. 地震波のスペクトル構造
—マグニチユードと卓越周期の関係—

地震研究所　松　本　利　松

光学的に記録された地震記象を 2 進化したテープに変換する変換装置を新に製作した．この進化した記録を以前に報告したリレー式相関計算器にかけ，フーリエ解析を行つた．

1958 年 4 月，金華山沖に群発した地震を筑波山において観測した記録を使い，P 波部分および S 波部分の速度スペクトルを 1 秒から 36 秒の帯域について計算した．解析時間は 36 秒，標本化の時間間隔は 0.2 秒である．

主な結果は次の通りである．

(1) 速度スペクトルは全体としては比較的平均した強度分布を持つている．

(2) 精密に見ると，スペクトルには数個の極大が認められる．これらの極大値は P 波部分については 3 群に，S 波部分については 2 群にわけられる．極大値に対する周期の対数をマグニチュードについてプロットすると，かなり見事に直線上にのり，これらの直線は互に平行している．

(3) 震源を球殻のモデルに置きかえ，第 1 種の振動について固有周期を計算した結果と比較すると，これらの周期の比は $n=2$, $N=0$ および 1 に対応する振動周期の比と一致する．ただし n, N の値は θ および半径の方向に対する節平面の数を表わす．

(4) マグニチュード卓越周期の観測結果および，卓越周期震源模型の半径の計算結果を組合わせて，マグニチュード震源模型の半径の関係が求められた．すなわち

$$M=0.02+3.97 \log a(\mathrm{km})$$

これは従来の地震体積などの計算と一致する．

(5) 基本周期および高調波の周期は震源模型の仮定によつてかなり影響されるので，発震機構の研究などにもこの高調波の解析は有効であろう．
